Hydrol. Earth Syst. Sci. Discuss., 7, 4219–4251, 2010
www.hydrol-earth-syst-sci-discuss.net/7/4219/2010/
doi:10.5194/hessd-7-4219-2010

Hydrology and
Earth System
Sciences
Discussions

Evaluation of global continental hydrology as simulated by the Land-surface Processes and eXchanges Dynamic Global Vegetation Model

S. J. Murray[1], **P. N. Foster**[1], **and I. C. Prentice**[1,2,3]

[1]QUEST, Department of Earth Sciences, Wills Memorial Building, University of Bristol, Queens Road, Bristol, BS8 1RJ, UK
[2]Department of Biological Sciences, Macquarie University, North Ryde, NSW 2109, Australia
[3]Grantham Institute of Climate Change, and Division of Biology, Imperial College, Silwood Park, Ascot, SL5 7PY, UK

Received: 22 June 2010 – Accepted: 28 June 2010 – Published: 6 July 2010

Correspondence to: S. J. Murray (steve.murray@bristol.ac.uk)

Published by Copernicus Publications on behalf of the European Geosciences Union.

Abstract

Global freshwater resources are sensitive to changes in climate, land cover and population density and distribution. The Land-surface Processes and eXchanges Dynamic Global Vegetation Model (LPX-DGVM) is a development of the Lund-Potsdam-Jena model with improved representation of fire-vegetation interactions. It allows simultaneous consideration of the effects of changes in climate, CO_2 concentration, natural vegetation and fire regime shifts on the continental hydrological cycle. Here the model is assessed for its ability to simulate large-scale spatial and temporal runoff patterns, in order to test its suitability for modelling future global water resources. Comparisons are made against observations of streamflow and a composite dataset of modelled and observed runoff (1986–1995).

The model captures the main features of the geographical distribution of global runoff, but tends to overestimate runoff in much of the Northern Hemisphere (where this can be largely accounted for by freshwater extractions and the unrealistic accumulation of the simulated winter snowpack in permafrost regions) and the southern tropics. Interannual variability is represented reasonably well at the large catchment scale, as are seasonal flow timings and monthly high and low flow events. Further improvements to the simulation of intra-annual runoff might be achieved via the addition of river flow routing. Overestimates of runoff in some basins could likely be corrected by the inclusion of transmission losses and direct-channel evaporation.

1 Introduction

Accurate representations of freshwater fluxes and their responses to global environmental change are needed in order to quantify the availability of global water supplies, particularly with regard to identifying regions susceptible to floods and droughts and for studies of global water resources in a changing world (e.g. Arnell, 1999, 2004; Lehner, 2006; Alcamo, 2007). Comprehensive assessments of the global water cycle require vegetation processes to be fully embedded in hydrological models (Cramer et al., 2001; Gerten et al., 2004). Increasingly advanced dynamic global vegetation models (DGVMs) are evolving into multi-purpose tools for representing land surface processes and feedbacks influencing the major components of the hydrological cycle (e.g. Gerten et al., 2004; Müller et al., 2006) and other exchanges of materials between the biosphere and the atmosphere (Arneth et al., 2010). However, so far DGVMs have been developed and evaluated primarily for their performance with respect to vegetation and biogeochemistry. Application of DGVMs to water resources questions requires that they be critically evaluated, and improved where necessary, using hydrological observations as the benchmark.

Interactions between vegetation and hydrology operate on micro to macro scales. For example, it is well established that vegetation regulates runoff at the macro scale via interception (Winsemius et al., 2005), changes in albedo (Mylne and Rowntree, 1992), transpiration (Levis et al., 2000) and land cover change (Bosch and Hewlett, 1982; Foley et al., 2005; D'Almeida et al., 2007). Influencing runoff at the micro level are reductions in stomatal conductance in response to increasing atmospheric carbon dioxide concentrations, resulting in a greater carbon dioxide intake per unit of water transpired (Gedney et al., 2006). This physiological effect has been proposed to account for a 6% increase in mean global runoff since pre-industrial times (Betts et al., 2007). However, its importance has been contested, as the physiological effects of carbon dioxide could lead to compensating increases in leaf area index (LAI) (Piao et al., 2007; Huntington, 2008). DGVMs attempt to resolve such discrepancies by quantifying the various competing processes and allowing them to work together. The extent to which they do so correctly can only be evaluated through extensive comparison with observations.

This paper aims to evaluate the macro-hydrological performance of a leading DGVM of intermediate complexity – LPX (Land-surface Processes and eXchanges: Prentice et al., 2010). LPX is the most recent development from the Lund-Potsdam-Jena (LPJ) model (Sitch et al., 2003) with improved hydrology as introduced by

Gerten et al. (2004). We compare simulated runoff fields against observations of global streamflow and an independent composite, model-adjusted runoff dataset.

Previous versions of LPJ have been evaluated with regard to carbon storages and fluxes (Sitch et al., 2003), soil moisture (Wagner et al., 2003), crop phenology (Bondeau et al., 2007) and hydrology (Gerten et al., 2004). Comparative evaluations of LPX and several other DGVMs, including two versions of LPJ, are underway for seasonal, interannual and interdecadal indicators of carbon cycling, water cycling and remotely sensed green vegetation cover (E. M. Blyth et al., personal communication, 2010). LPJ has been shown to perform reasonably well in comparison to similar models at both the basin scale (thirteen US basins; Gordon et al., 2004) and the global scale (Cramer et al., 2001). In the former study, however, it was shown that models which prescribe vegetation generally tend to generate more reliable hydrology than DGVMs. Gerten et al. (2004) reported that runoff and evaporation agree well with comparable hydrological models, although considerable discrepancies in runoff estimation persisted in some regions, particularly in the tropics.

2 Methods

2.1 The LPX Model

LPX simulates global biospheric dynamics through process-based representations of biogeochemical and biogeophysical processes at the land surface at 0.5° spatial resolution, using nine plant functional types (PFTs). An in-depth discussion of carbon allocation and vegetation establishment was presented by Sitch et al. (2003) in LPJ, while terrestrial biosphere parameter uncertainties have been considered by Zaehle et al. (2005). Gerten et al. (2004) detailed the hydrological process representations, which are briefly summarised here.

Runoff is determined as net precipitation (after interception) minus transpiration from two soil layers and surface evaporation from the top soil layer (Gerten et al., 2004).

There is no built-in river routing algorithm so any runoff generated is assumed to reach the basin outlet at the end of each model day. Soil moisture is the water remaining after transpiration, evaporation, infiltration and runoff have been accounted for. Potential evaporation is calculated based on the Priestley-Taylor equation (Priestley and Taylor, 1972; Hobbins et al., 2001). Transpiration is the lesser of an atmospheric demand term (which combines potential evaporation and surface conductance, following Monteith (1995)) and a soil/plant moisture supply term (a maximal rate determined by plant hydraulic properties, reduced as a function of declining soil moisture content).

2.2 Data

A global gridded model-observation composite dataset and two river discharge observation datasets are used to evaluate LPX simulated runoff, in addition to estimates of freshwater extractions.

Global observations of monthly runoff are relatively sparse and discrepancies in monitoring frequency, quality and technique combine to make it difficult to synthesise such data in a common format and assess their reliability. One source of global gridded runoff is a product of the ISLSCP II project: the UNH-GRDC Composite Global Runoff Fields (Fekete et al., 1999, 2002). This represents a combination of climate-driven water balance runoff model (WBM) outputs and Global Runoff Data Centre (GRDC) observed river discharge observations for the period 1986–1995, on a monthly basis at 0.5° resolution. Observations account for 72% of the actively discharging (> 3 mm/year) global land area (Fekete et al., 2002). River discharge measured at a point and WBM-simulated runoff are disaggregated between pre-defined interstation domains and corrected according to observations (Fekete et al., 2002). Monthly outputs are adjusted via annual corrections to account for mistimings in intra-annual runoff which may arise as a result of storage in excess of a month (Fekete et al., 1999).

Observations of mean monthly global river discharge provided by the GRDC are also used to evaluate runoff for the twelve largest catchments in the world by area (O'Connor and Costa, 2004). Data from the furthest downstream gauging station have been selected, since this should approximate aggregated catchment runoff. While such measurements are usually estimated to incur error in magnitude of between 5–10% (Rantz, 1982) and up to 20% (Hageman and Dümenil, 1998; Dingman, 2001), these data should still offer a solid alternative against which to benchmark simulated runoff, with the advantage of being independent of any model.

A dataset of monthly river discharge for 1948–2004 from 925 global rivers, accounting for ~ 73% of global streamflow (Dai et al., 2009) is used to evaluate LPX interannual variability in runoff. Data are predominantly composed of observations, from GRDC, UNH and NCAR archives, but where gaps in the time-series or unmonitored regions exist, these are infilled by using nearby gauges and the Community Land Model, version 3 (CLM3; Oleson et al., 2004).

Water extractions from rivers and aquifers are based on Oki et al. (2001). Oki et al. use population distribution and irrigated land area (assumed proportional to municipal, industrial and agricultural extractions respectively) to form 0.5° global gridded annual estimates of water usage for 1995. These data are compiled from various sources at the country-scale (WRI, 1998) for varying time periods and linearly adjusted to determine values for the target year.

2.3 Model set-up

A spin-up period was used to initialise the model, which was forced with input variables detrended using the lowess technique. The 1961–1990 period was recycled at 286 ppm CO_2 until the thirty year means of the slow carbon pools varied by $< 2\%$ for each grid cell. LPX was subsequently run for 1850–2006, forced with 0.5° monthly gridded fields of air temperature, precipitation, wet day frequency and cloud cover fraction from the Climate Research Unit (CRU) TS 3.0 archive (e.g. Mitchell and Jones, 2005) along with global annually varying CO_2 concentrations (Etheridge et al., 1996; IPCC, 2001) and nine fixed soil texture types (Zobler, 1986). Fractional sunshine hours data range from 1901–2002, with 1997–1998 formed of monthly means from the previous thirty years and beyond 2002 composed of converted sun hour observations and synthetic data derived from daily temperature ranges. Wet day data are determined from a combination of station measurements and synthetic wet days derived from precipitation, while being entirely synthetically-derived from precipitation from 1990 onwards.

3 Results

3.1 Key features and data-model comparisons

3.1.1 Trend

LPX simulated runoff shows a decrease of 0.12 mm/year through the period 1951–2000 (Fig. 1). Simulated variations in global runoff over the 20th century compare well with the reconstruction of Dai et al. (2009), in terms of most interannual variability features and the presence of a decreasing trend for 1951–2000 being captured. However, the trend as simulated by LPX is steeper than in the Dai et al. (2009) data set.

The trend of the CRU terrestrial precipitation data used here is slight and in agreement with GHCN data for the latter half of the 20th century (Bosilovich et al., 2005). Downward trends as shown in the Dai et al. (2009) data set, and simulated by LPX, therefore must have other causes, e.g. increasing leaf area index (Piao et al., 2007) leading to increased evaporative losses.

3.1.2 Interannual variability

LPX tracks the interannual variability of the composite global mean and Dai reconstructions very well, although the absolute values of runoff are overestimated by between 65–88 mm/year and 33–76 mm/year respectively, probably at least in part due to water abstractions not considered in the DGVM. The interannual variability in runoff appears to be explained largely via changes in precipitation for LPX ($r = 0.56$; $p \approx 0$), Dai reconstructions ($r = 0.50$; $p \approx 0$), and the ISLSCP II composite ($r = 0.71$; $p = 0.02$).

3.1.3 Comparison to other models

LPX performs well when related to other similar models for simulation performance, using the Willmott Index of Agreement (Willmott, 1982). This is a metric of simulation quality based on the mean and variance of the outputs compared to their associated observations, whereby 1 = perfect agreement between simulations and observations, and 0 = complete disagreement. When tested for interannual variability against the Dai reconstructions and ISLSCP II composite data, LPX scores 0.98 and 0.92 respectively compared to a range of 0.89 (for Gerten-LPJ) to 0.92 ("Model 2") as reported in Gerten et al. (2004). The global mean absolute deviation (bias) for LPX is 60 mm/year for the Dai reconstructions and 74 mm/year for ISLSCP II, compared to a range of −1471 ("Model 1") to 442 mm/year ("Model 3") for 663 catchments. LPX total global annual runoff averaged for the period 1961–1990 is 56 865 km^3/year from a land area of 128×10^6 km^2, compared to 37 288 km^3/year for Dai et al. (2009) from an area of 117×10^6 km^2 (Dai and Trenberth, 2002), and 37 075 km^3/year from an area of 112×10^6 km^2 for the ISLSCP II composite data. Incorporation of total global annual freshwater extractions of 3448 km^3/year for 1995 (according to Oki et al., 2001) results in a revised estimate of 53 417 km^3/year. Previous estimates range from ~ 36 500 km^3 (Chanine, 1992) to ~ 45 500 km^3 (Cogley, 1991) while Gerten et al. (2004) estimated total runoff as being 40 143 km^3. LPX thus predicts global annual total runoff in excess of previous estimates.

3.1.4 Global runoff distribution

LPX captures the global runoff distribution well, but has a general tendency to overestimate runoff magnitude, particularly in the tropics and throughout much of the Northern Hemisphere, while underestimations are typical surrounding the equator (Fig. 2). These discrepancies are most likely born out of an imbalance in the simulated precipitation-evaporation ratio. The findings described here compare favourably to similar studies by Sitch et al. (2003) and Gerten et al. (2004) with regard to the relative magnitudes of runoff across latitudinal domains, when validated against observations and macro-scale hydrological models, although the former has a bias towards underestimation of runoff.

The incorporation of extractions (based on 1995 data) considerably improves the simulation of runoff between 20–55° N in such that LPX then closely resembles the composite runoff distribution. The largest overestimations still remain in the southern tropics, where extractions are less substantial. It should be acknowledged that a greater proportion of streamflow observations exist in Europe, North America, South America and parts of western Africa, where the river gauge network density is highest (Fekete et al., 2002). ISLSCP II runoff data incorporate freshwater extractions in such regions and thus represent a more suitable runoff comparator. Uncertainty in runoff evaluation is greater in regions where ISLSCP II runoff is model-generated, and particularly where population densities are high, due to the omission of water withdrawals.

LPX shows considerable overestimations of annual runoff throughout much of Central and Northern America, parts of South America, the tropics of Africa, south and eastern Asia and eastern Europe (Fig. 3a). Underestimations are largely restricted to equatorial regions, central Europe, the UK, and the northernmost latitudes. LPX best represents annual runoff in the Sahel, central and western Asia, parts of North America, south-western South America and southern Australia. These findings are generally consistent with those of Gerten et al. (2004) using LPJ, with improvements apparent in the north-west of North America and some parts of semi-arid northern Africa.

When including freshwater extractions (Fig. 3b and c), LPX shows a considerable reduction in the overestimates for much of Europe, North America and East Asia. Some regions of China, India and the mouth of the Nile river, where runoff is overestimated by LPX, are shown to be underestimated when withdrawals are incorporated.

3.1.5 Interannual variability at the catchment scale

LPX grid cells that fall within the boundaries of the selected river catchments (GRDC, 2007) have been used to test interannual variability. The model tends to perform well in replicating trends and is often within, or close to the periphery of the runoff envelope shown by the composite and monthly summed converted river discharge data (Fig. 4). For the basins being tested, LPX best represents the interannual runoff of the Amazon, Amur, Yenisei, Lena and Zambezi, and represents the Congo well with respect to the composite data. Runoff for the other catchments tends to be overestimated, particularly for the Nile, Mississippi, Parana and Niger. Of the catchments which are coincident with those validated by Gerten et al. (2004), albeit for different time periods, LPX better simulates interannual variability of runoff for the Amazon, Nile and Yenisei, but more greatly overestimates for the Congo and Mississippi.

The inclusion of water extractions for 1995 either improves or does not adversely affect the simulation of runoff in most catchments, especially the Mississippi. The one exception is the Yangtze, where extractions cause simulated runoff to fall below the ISLSCP II estimate. Cases where runoff still remains in excess of observations, in spite of extraction being included (e.g. the Nile, Amur, Parana, Niger and Zambezi catchments) may be due to the absence of river routing and human infrastructure (most notably dams) from the model, causing flow impedances and enhanced evaporation to be overlooked.

3.1.6 Seasonal variability at the catchment scale

While the seasonality of flows is generally well represented by LPX at the catchment scale, there is a tendency towards early estimation of the extremes of runoff by at least a month (Fig. 5). The greater discrepancies lie in the magnitudes of summed monthly flow. With the exception of the Amur, Yenisei and Yangtze, LPX does not replicate the peaks in runoff as seen in the river discharge records. Gerten et al. (2004) report broadly similar findings for the coincident catchments (for differing time periods), although LPX better represents the seasonal peak of the Yenisei and achieves a slightly better, but still poor, replication of intra-annual flow in the Nile. However, monthly flow timings in the Mississippi are better captured by the former version of the model. Simulated runoff generally tracks CRU TS 3.0 intra-annual precipitation due to the assumption of runoff being generated and outputted from the basin within a given day. As a result, the model tends to overlook the multiple runoff regulators present in river catchments, causing the timings of simulated peak flows to generally be out of synchrony with observations. The ISLSCP II composite data, which are formed via a simple routing mechanism of runoff within the WBM (Fekete et al., 1999), fare little better in demonstrating accurate flow timings in comparison to LPX. However, while LPX is more likely to overestimate the runoff from northern latitude catchments, Gerten et al. (2004) note a deficit in comparison to observations, which is attributed to systematic errors in high-latitude precipitation data, and the simplistic model representation of snow accumulation and melt.

3.1.7 Global flow timings

At the individual cell scale, LPX has a slight propensity towards late prediction of global peak intra-annual flow (mean difference of 0.068 months compared to the composite dataset, in contrast to ~ 1 month early with the former version of LPJ: Gerten et al. (2004)), although there are notable regional differences (Fig. 6a, b and c). The Sahel, Arabian Peninsula, central North America, central Asia and parts of central Africa are most poorly captured, due to the difficulty associated with discerning non-routed monthly runoff maximums in consistently dry climates (and especially since the extremities of the annual hydrographs are dampened due to the absence of channel evaporation and transmission loss processes from the model). Aside from these notable exceptions, the maximum month of runoff is generally well simulated for most of the Northern Hemisphere. The Southern Hemisphere shows a bias towards a slight early estimation of runoff.

3.2 Comparison with various indices of drought

The reliable forecasting of droughts is critical to all simulations of global water resources. Unlike flooding, the definition of drought is not agreed, due to differing perceptions of water shortage magnitude and duration between regions (e.g. Dracup et al., 1980). Broadly one can distinguish meteorological drought (shortages of precipitation), hydrological drought (shortages of runoff and/or streamflow), agricultural or ecological drought (soil moisture shortages) and socio-economic drought (a shortage of water to support consumptive economic demand) (Keyantash and Dracup, 2002). This section focuses on the simulation of the physical forms of drought and the application of hydrological statistics to assess high and low flows.

3.2.1 Comparison of LPX to the Palmer Drought Severity Index

LPX annual and monthly runoff is compared to the Palmer Drought Severity Index (PDSI; Palmer, 1965). The PDSI is a hybrid index based on antecedent precipitation, moisture supply and demand (following Thornthwaite, 1948; Dai et al., 2004). The index is most effective on an annual basis, while interpretation of monthly soil moisture values for northern latitudes requires caution due to the exclusion of snow accumulation and potential evaporation being assumed (according to Thornthwaite (1948)). However, the PDSI has been shown to correlate with soil moisture content during warm seasons in Illinois and Eurasia, and streamflow from large global catchments (Dai et al., 2004). Regional-scale studies of recent and historical droughts have been conducted using the PDSI (e.g. Karl, 1986; Lloyd-Hughes and Saunders, 2002; Fye et al., 2003; Ntale and Gan, 2003), while Dai et al. (1998) also used this index to estimate the influence of the El Niño-Southern Oscillation on global variability in wet and dry periods.

With the exception of the final years of the twentieth century, the direction of the PDSI trend, in showing a global tendency towards drying, is reproduced by LPX (Fig. 7). Interannual variability is also generally captured well, but with runoff and precipitation preceding the PDSI by a year in some cases. LPX runoff ($r = 0.49$; $p = 0.001$) replicates the PDSI trend much better than precipitation alone ($r = -0.0009$; $p = 0.995$).

3.2.2 Comparison of LPX with high and low flow observations

In order to determine the suitability of LPX as a tool for predicting future shortage and surplus in the regional water budget, LPX summed total catchment monthly runoff is compared against GRDC runoff-equivalent monthly river discharge (GRDC, 2007) for a selection of large catchments on a per-event basis.

LPX consistently overestimates monthly peak flows in the Mississippi catchment (possibly due to the omission of human abstractions), and often mistimes high flows by a month (Fig. 8; $r = 0.57$; $p \approx 0$). The Mississippi flood of 1973 (e.g. Deutsch and Ruggles, 1974; Chin et al., 1975) is reproduced by LPX but at three times the peak magnitude and two months early. There is also a tendency to overestimate low flow events while some timings are incongruent. Peak flow magnitudes are represented much more successfully for the Yangtze catchment, while low flows are underestimated (Fig. 8; $r = 0.76$; $p \approx 0$). Flow timings are generally well simulated, but sometimes disparate by a month. The Yenisei is captured very well with regard to the simulation of peak flow magnitudes and timings (Fig. 8; $r = 0.87$; $p \approx 0$), but again, while low flow timings are modelled well, event magnitudes are consistently underestimated. Overall however, peak and low flow timings are generally well captured for the catchments tested, and reasonable simulations of flow magnitudes are shown.

3.2.3 Simulation of high flows and various forms of droughts

Basin sums of monthly LPX runoff, GRDC observed streamflow (converted to mm/month) and CRU TS 3.0 precipitation are used to assess the simulation of hydrological and meteorological drought respectively. Agricultural or ecological drought is evaluated using gravimetric soil moisture observation point data from the Global Soil Moisture Data Bank (GSMDB; Robock et al., 2000) for river catchments in Russia. Data are available for the upper 1 m soil layer of natural grass plots of ~ 0.1 ha for 1978–1985. These have been formed by averaging four measurement points in each plot every 10 days during the growing season and once per month during winter

(Robock et al., 2000). Monthly means have subsequently been created for each of the Amur (11 soil moisture stations), Lena (17 stations) and Ob (13 stations) catchments.

In order to assess the ability of the model to capture varying forms of drought, statistical metrics are used as a means to characterise high and low flows. Q95 (the number of months in which flow magnitude is exceeded 95% of the time; low flows) and Q5 (flow exceeded 5% of the time; high flows) metrics are applied to each variable for each basin (Table 1).

LPX appears capable of capturing all forms of physical high flows (with the exception of soil moisture in cases where observations are limited). Low flows are reasonably well captured, with hydrological "droughts" simulated most accurately.

Variability in the magnitude of LPX monthly runoff generally mimics that of precipitation, river discharge and soil moisture (Fig. 9). The spring melt is consistently overestimated and in some cases simulated runoff exceeds precipitation (particularly in the Lena and Ob catchments), while always exceeding GRDC river discharge. This problem occurs due to the simulated accumulation of winter precipitation into the snowpack when monthly temperatures are $< 0\,^{\circ}$C (Gerten et al., 2004). Daily infiltration when temperatures exceed $0\,^{\circ}$C is omitted, causing LPX spring runoff to also exceed observed river discharge when this enhanced winter storage melts.

4 Discussion and conclusions

LPX is able to adequately capture the global distribution of runoff, interannual and seasonal runoff variability at the continental and catchment scale, and represents high and low flows reasonably well in large catchments. Several factors can induce a lag in the arrival of water at the catchment outlet (Kuhl and Miller, 1992; Costa and Foley, 1999), highlighting the need to include water routing in DGVMs (Marengo et al., 1994). Some overestimations (particularly between 20–55° N) can be accounted for by water extractions. However, errors in the precipitation data (e.g. Fekete et al., 2004; Biemans et al., 2009) may also be involved. Widespread overestimation of runoff may also be attributed in part to LPX underestimating global rainfall interception (Murray, 2010).

Aside from the Yenisei, the poor agreement in runoff extremes and timing for the high latitude catchments is likely due to simplified representation of snow accumulation and melt dynamics, in addition to the absence of permafrost in the model. The incorporation of a glacial mass-balance component into the DGVM may bring improvements.

LPX, in common with many hydrological models (e.g. Döll et al., 2003) is unable to reproduce the interannual and seasonal peak in runoff observed in semi-arid catchments such as the Nile and Niger. The Niger and Nile are unusual cases in that beyond a point, discharge decreases with distance downstream. For example, approximately half of the Nile's annual flow is lost from the Sudd marshes via evaporation (including that directly from the channel) and transmission losses (Ibrahim, 1984). Commonly overlooked in global hydrological modelling, transmission losses must be considered in order for simulations to perform well in dry catchments.

Wet and dry periods are represented reasonably well through comparison at the global scale to the PDSI. In addition, high and low flow events are generally simulated well for the Mississippi, Yangtze and Yenisei, and flow event timings are generally captured very well. High and low flows are modelled well and various forms of drought are simulated reasonably. Spring melt in the selected Russian basins is considerably overestimated due to the unrealistic accumulation of the winter snowpack.

Various factors not incorporated in the DGVM may contribute to differences between observed and simulated water fluxes. Most critically, monitored river discharge is often subject to significant human abstractions (e.g. Döll et al., 2009). The exclusion of such an important component of estimated global river flows from DGVMs and hydrological models leads to consistent overestimation of runoff in populated catchments. The absence of wetlands and dams in the model affects both the peaks in flow rate and volume of discharge retained, and could be improved via inclusion of flow routing (e.g. Olivera et al., 2000; Oki et al., 2001). In some cases, discrepancies might be attributed to the unavailability of river discharge data to match the period of simulated runoff, or to the fact that the gauging stations are not situated at the most distal point of the river. Further improvement of the hydrological element of LPX will require the inclusion of human abstractions and a flow routing scheme, and the representation of transmission and direct-channel evaporation losses (particularly in semi-arid regions). Such additions to the DGVM should produce a step-change improvement to global runoff modelling and will facilitate the application of LPX as a tool for flood and drought prediction.

Acknowledgements. S. J. Murray is the beneficiary of a doctoral grant from the AXA Research Fund. This research is also supported by the European Union Sixth Framework Programme project Hydrogen, Methane, Nitrous Oxide (HYMN), the NERC programme Quantifying and Understanding the Earth System (QUEST) and the European Union Seventh Framework project Comprehensive Modelling of the Earth System for Climate Better Prediction and Projection (COMBINE).

References

Alcamo, J., Flörke, M., and Märker, M.: Future long-term changes in global water resources driven by socio-economic and climatic changes, Hydrolog. Sci. J., 52, 2, 247–275, 2007.

Arnell, N. W.: The effect of climate change on hydrological regimes in Europe: A continental perspective, Sci. Tech., 9, 5–23,1999.

Arnell, N. W.: Climate change and global water resources: SRES emissions and socio-economic scenarios, Sci. Tech., 14, 31–52, 2004.

Arneth, A., Sitch, S., Bondeau, A., Butterbach-Bahl, K., Foster, P., Gedney, N., de Noblet-Ducoudré, N., Prentice, I. C., Sanderson, M., Thonicke, K., Wania, R., and Zaehle, S.: From biota to chemistry and climate: towards a comprehensive description of trace gas exchange between the biosphere and atmosphere, Biogeosciences, 7, 121–149, doi:10.5194/bg-7-121-2010, 2010.

Betts, R. A., Boucher, O., Collins, M., Cox, P. M., Falloon, P. D., Gedney, N., Hemming, D. L., Huntingford, C., Jones, C. D., Sexton, D. M. H., and Webb, M. J.: Projected increase in continental runoff due to plant responses to increasing carbon dioxide, Nature, 448, 1037–1042, 2007.

Biemans, H., Hutjes, R. W. A., Kabat, P., Strengers, B. J., Gerten, D., and Rost, S.: Effects of precipitation uncertainty on discharge calculations for main river basins, J. Hydrometeorol., 10, 1011–1025, 2009.

Bondeau, A., Smith, P., Zähle, S., Schaphoff, S., Lucht, W., Cramer, W., Gerten, D., Lotze-Campen, H., Müller, C., Reichstein, M., and Smith, B.: Modelling the role of agriculture for the 20^{th} century, Glob. Change Biol., 13, 679–706, 2007.

Bosch, J. M. and Hewlett, J. D.: A review of catchment experiments to determine the effect of vegetation changes on water yield and evapotranspiration, J. Hydrol., 55, 3–23, 1982.

Bosilovich, M. G., Schubert, S. D., and Walker, G. K.: Global changes of the water cycle intensity, J. Climate., 18, 10, 1591–1608, 2005.

Chanine, M. T.: The hydrological cycle and its influence on climate, Nature, 359, 373–380, 1992.

Chin, E. H., Skelton, J., and Guy, H. P.: The 1973 Mississippi River basin flood: compilation and analysis of meteorologic, streamflow and sediment data, US Geological Survey Professional Paper 937, 137 pp., 1975.

Cogley, J. G.: GGHYDRO – Global Hydrographic Data Release 2.0, Department of Geography, Trent University, 1991.

Costa, M. H. and Foley, J. A.: Trends in the hydrologic cycle of the Amazon basin, J. Geophys. Res., 104, 14189–14198, 1999.

Cramer, W., Bondeau, A., Woodward, F. I., Prentice, I. C., Betts, R. A., Brovkin, V., Cox, P. M., Fisher, V., Foley, J. A., Friend, A. D., Kucharik, C., Lomas, M. R., Ramankutty, N., Sitch, S., Smith, B., White, A., and Young-Molling, C.: Global response of terrestrial ecosystem structure and function to CO_2 and climate change: Results from six dynamic global vegetation models, Glob. Change Biol., 7, 357–373, 2001.

Dai, A. G, Trenberth, K. E., and Karl, T. R.: Global variations in droughts and wet spells: 1900–1995, Geophys. Res. Lett., 25, 3367–3370, 1998.

Dai, A. and Trenberth, K. E.: Estimates of freshwater discharge from continents: latitudinal and seasonal variations, J. Hydrometeorol., 3, 660–687, 2002.

Dai, A., Trenberth, K. E., and Qian, T.: A global data set of Palmer Drought Severity Index for 1870–2002: relationship with soil moisture and effects of surface warming, J. Hydrometeorol., 5, 1117–1130, 2004.

Dai, A., Qian, T., and Trenberth, K. E.: Changes in continental freshwater discharge from 1948 to 2004, J. Climate., 22, 2773–2792, 2009.

D'Almeida, C., Vörösmarty, C. J., Hurtt, G. C., Marengo, J. A., Dingman, S. L., and Keim, B. D.: The effects of deforestation on the hydrological cycle in Amazonia: a review on scale and resolution, Int. J. Climatol., 27, 633–647, 2007.

Deutsch, M. and Ruggles, F.: Optical data processing and projected applications of the ERTS-1 imagery covering the 1973 Mississippi river valley floods, J. Am. Water Resour. As., 10, 5, 1023–1039, 1974.

Dingman, S. L.: Physical Hydrology, Prentice-Hall, Englewood Cliffs, N.J., 2001.

Döll, P., Kaspar, F., and Lehner, B.: A global hydrological model for deriving water availability indicators: model tuning and validation, J. Hydrol., 270, 105–134, 2003.

Döll, P., Fiedler, K., and Zhang, J.: Global-scale analysis of river flow alterations due to water withdrawals and reservoirs, Hydrol. Earth Syst. Sci., 13, 2413–2432, doi:10.5194/hess-13-2413-2009, 2009.

Dracup, J. A., Lee, K. S., and Paulson Jr., E. G.: On the definition of droughts, Water Resou. Res., 16, 2, 297–302, 1980.

Etheridge, D., Steele, L., Langenfelds, R., Francey, R., Barnola, J.-M., and Morgan, V.: Natural and anthropogenic changes in atmospheric CO_2 over the last 1000 years from air in Antarctic ice and firn, J. Geophys. Res., 101, D2, 4115–4128, 1996.

Fekete, B. M., Vörösmarty, C. J., and Grabs, W.: Global, Composite Runoff Fields Based on Observed River Discharge and Simulated Water Balances, GRDC Report 22, Global Runoff Data Center, Koblenz, Germany, 1999.

Fekete, B. M., Vörösmarty, C. J., and Grabs, W.: High resolution fields of global runoff combining observed river discharge and simulated water balances, Global Biogeochem. Cy., 16(3), 1042, doi:10.1029/1999GB001254, 2002.

Fekete, B. M., Vörösmarty, C. J., Roads, J. O., and Willmott, C. J.: Uncertainties in precipitation and their impacts on runoff estimates, J. Climate, 17, 2, 294–304, 2004.

Foley, J. A., DeFries, R., Asner, G. P., Barford, C., Bonan, G., Carpenter, S. R., Chapin, F. S., Coe, M. T., Daily, G. C, Gibbs, H. K., Helkowski, J. H., Holloway, T., Howard, E. A., Kucharik, C. J., Monfreda, C., Patz, J. A., Prentice, I. C., Ramankutty, N., and Snyder, P. K.: Global consequences of land use, Science, 309, 570–574, 2005.

Fye, F. K., Stahle, D. W., and Cook, E. R.: Paleoclimatic analogs to twentieth-century moisture regimes across the United States, B. Am. Meteorol. Soc., 84, 901–909, 2003.

Gedney, N., Cox, P. M., Betts, R. A., Boucher, O., Huntingford, C., and Scott, P. A.: Detection of a direct carbon dioxide effect in continental river runoff records, Nature, 439, 835–838, 2006.

Gerten, D., Schaphoff, S., Haberlandt, U., Lucht, W., and Sitch, S.: Terrestrial vegetation and water balance – hydrological evaluation of a dynamic global vegetation mode, J. Hydrol., 286, 249–270, 2004.

Global Runoff Data Centre: Major river basins of the world, GRDC in the Bundesanstalt fuer Gewaesserkunde, 56068 Koblenz, Germany, http://grdc.bafg.de, 2007.

Gordon, W. S., Famiglietti, J. S., Fowler, N. L., Kittel, T. G. F., and Hibbard, K. A.: Validation of simulated runoff from six terrestrial ecosystem models: results from VEMAP, Ecol. Appl., 14, 527–545, 2004.

Hagemann, S. and Dümenil, L.: A parameterization of the lateral waterflow for the global scale, Clim. Dynam., 14, 17–31, 1998.

Hobbins, M. T., Ramírez, J. A., and Brown, T. C.: The complementary relationship in estimation of regional evapotranspiration: an enhanced advection-aridity model, Water Resour. Res., 37, 1389–1403, 2001.

Huntington, T. G.: CO_2-induced suppression of transpiration cannot explain increasing runoff, Hydrol. Process., 22, 311–314, 2008.

Ibrahim, A. M.: The Nile: Description, hydrology, control and utilisation, Hydrobiologia, 110, 1, 1–13, 1984.

IPCC: Appendix II – SRES Tables in Climate Change 2001: The Scientific Basis. Contribution of Working Group I to the Third Assessment Report of the Intergovernmental Panel on Climate Change, edited by: Houghton, J. T., Ding, Y., Griggs, D. J., Noguer, M., van der Linden, P. J., Dai, X., Maskell, K., and, Johnson, C. A., Cambridge University Press, Cambridge, United Kingdom and New York, NY, USA, 881 pp., 2001

Karl, T. R.: Sensitivity of the Palmer Drought Severity Index and Palmer's Z-index to their calibration coefficients including potential evapotranspiration, J. Clim. Appl. Meteorol., 25, 77–86, 1986.

Keyantash, J. and Dracup, J. A.: The quantification of drought: an evaluation of drought indices, B. Am. Meteorol. Soc., 83, 1167–1180, 2002.

Kuhl, S. C. and Miller, J .R.: Seasonal river runoff calculated from a global atmospheric model, Water Resour. Res., 28, 2029–2039, 1992.

Lehner, B., Döll, P., Alcamo, J., Henrichs, T., and Kaspar, F.: Estimating the impact of global change on flood and drought risks in Europe: a continental, integrated analysis, Climatic Change, 75, 273–299, 2006.

Levis, S., Foley, J. A., and Pollard, D.: Large-scale vegetation feedbacks on a doubled CO_2 climate, J. Climate., 13, 1313–1325, 2000.

Lloyd-Hughes, B. and Saunders, M. A.: A drought climatology for Europe, Int. J. Climatol., 22, 1571–1592, 2002.

Marengo, J. A., Miller, J. R., Russell, G. L., Rosenzweig, C. E., and Abramopoulos, F.: Calculation of river runoff in the GISS GCM: Impact of a new land-surface parameterization and river routing model on the hydrology of the Amazon River, Clim. Dynam., 10, 349–361, 1994.

Mitchell, T. D. and Jones, P. D.: An improved method of constructing a database of monthly climate observations and associated high-resolution grids, Int. J. Climatol., 25, 6, 693–712, 2005.

Murray, S .J.: Trends in 20th century global rainfall interception as simulated by a Dynamic Global Vegetation Model: implications for global water resources, J. Hydrol., submitted, 2010.

Müller, C., Bondeau, A., Lotze-Campen, H., Cramer, W., and Lucht, W.: Comparative impact of climatic and nonclimatic factors on global terrestrial carbon and water cycles, Global Biogeochem. Cy., 20, GB4015, doi:10.1029/2006GB002742, 2006.

Mylne, M. F. and Rowntree, P. R.: Modelling the effects of albedo change associated with tropical deforestation, Climatic Change, 21, 1573–1480, 1992.

Ntale, H. K. and Gan, T. Y.: Drought indices and their application to East Africa, Int. J. Climatol., 23, 1335–1357, 2003.

O'Connor, J. E. and Costa, J. E.: The world's largest floods, past and present: their causes and magnitudes, US Geological Survey Circular 1254, 13 pp., 2004.

Oki, T., Agata, Y., Kanae, S., Saruhasi, T., Yang, D., and Musiake, K.: Global assessment of current water resources using total runoff integrating pathways, Hydrolog. Sci. J., 46, 983–995, 2001.

Oleson, K. W., Dai, Y., Bonan, G., Bosilovich, M., Dickinson, R., Dirmeyer, P., Hoffman, F., Houser, P., Levis, S., Niu, G.-Y., Thornton, P., Vertenstein, M., Yang, Z.-L., and Zeng, X.: Technical description of the Community Land Model (CLM), NCAR Technical Note NCAR/TN-4611STR, 186 pp., 2004.

Olivera, F., Famiglietti, J., and Asante, K.: Global scale flow routing using a source-to-sink algorithm, Water Resour. Res., 36, 2197–2207, 2000.

Piao, S., Friedlingstein, P., Ciais, P., de Noblet-Ducoudré, N., Labat, D., and Zaehle, S.: Changes in climate and land use have a larger direct impact than rising CO_2 on global river runoff trends, P. Natl. Acad. Sci. USA, 104, 15242–15247, 2007.

Prentice, I. C., Kelley, D. I., Foster, P. N., Friedlingstein, P., Harrison, S. P., and Bartlein, P. J.: Fire variability and the terrestrial carbon balance, Global Biogeochem. Cy., submitted, 2010.

Priestley, C. H. B. and Taylor, R. J.: On the assessment of surface heat flux and evaporation using large-scale parameters, Mon. Weather Rev., 100, 81–92, 1972.

Rantz, S. E.: Measurement and Computation of Streamflow, Vol. 2, Computation of Discharge, water-supply paper, 2175, US Geological Survey, Reston, VA, 1982.

Robock, A., Vinnikov, K. Y., Srinivasan, G., Entin, J. K., Hollinger, S. E., Speranskaya, N. A., Liu, S., and Namkhai, A.: The Global Soil Moisture Data Bank, B. Am. Meteorol. Soc., 81, 1281–1299, 2000.

Sitch, S., Smith, B., Prentice, I. C., Arneth, A., Bondeau, A., Cramer, W., Kaplan, J. O., Levis, S., Lucht, W., Sykes, T. M., Thonicke, K., and Venevsky, S.: Evaluation of ecosystem dynamics, plant geography and terrestrial carbon cycling in the LPJ dynamic global vegetation model, Glob. Change Biol., 9, 161–185, 2003.

Thornthwaite, C. W.: An approach toward a rational classification of climate, Geogr. Rev., 38, 55–94, 1948.

Wagner, W., Scipal, K., Pathe, C., Gerten, D., Lucht, W., and Rudolf, B. Evaluation of the agreement between the first global remotely sensed soil moisture data with model and precipitation data, J. Geophys. Res., 108, D19, 4611, doi:10.1029/2003JD003663, 2003.

Willmott, C. J.: Some comments on the evaluation of model performance, B. Am. Meteorol. Soc., 63, 1309–1313, 1982.

Winsemius, H. C., Savenije, H. H. G., Gerrits, A. M. J., Zapreeva, E. A., and Klees, R.: Comparison of two model approaches in the Zambezi river basin with regard to model reliability and identifiability, Hydrol. Earth Syst. Sci., 10, 339–352, doi:10.5194/hess-10-339-2006, 2006.

Zobler, L.: A world soil file for global climate modelling, NASA Technical Memorandum 87802, NASA/GISS, New York, USA, 32 pp., 1986.

Table 1. Q5 and Q95 monthly totals of summed monthly LPX runoff, GRDC river discharge, CRU TS 3.0 precipitation and mean GSMDB soil moisture for three Russian catchments.

	Runoff		River Discharge		Precipitation		Soil Moisture	
	Q5	Q95	Q5	Q95	Q5	Q95	Q5	Q95
Amur	1	53	4	71	3	72	46	95
Lena	1	40	1	43	1	80	42	95
Ob	1	52	1	68	2	89	2	93

Title Page
Abstract
Introduction
Conclusions
References
Tables
Figures
◄◄
►►
◄
►
Back
Close
Full Screen / Esc
Printer-friendly Version
Interactive Discussion

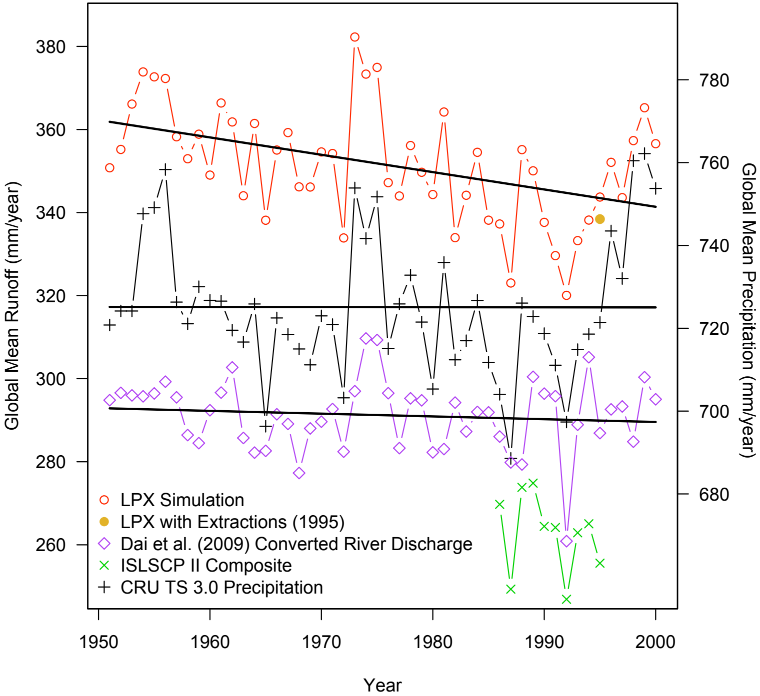

Fig. 1. Global Mean Annual Runoff as simulated by LPX for 1951–2000 (with freshwater extractions for 1995) and as represented by the ISLSCP II composite dataset for 1986–1995 in relation to global mean annual precipitation.

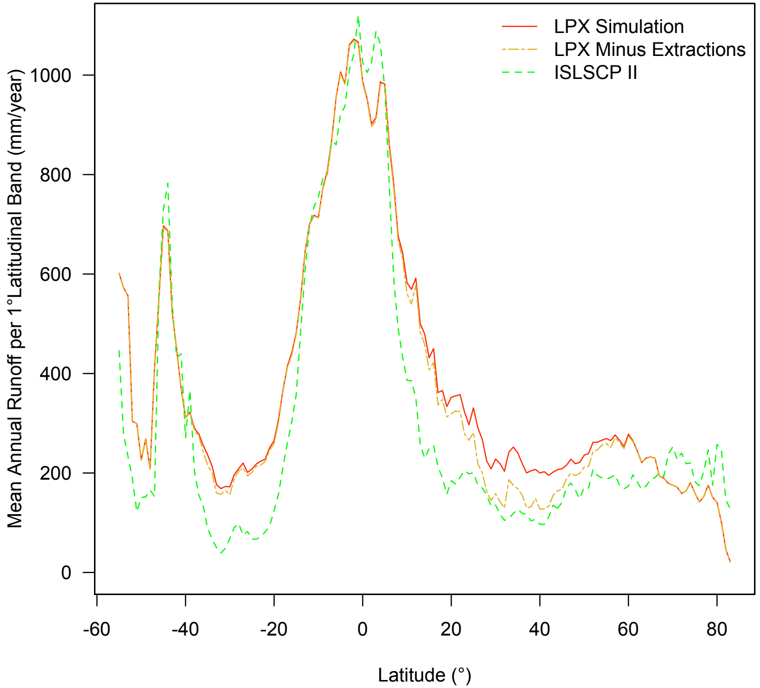

Fig. 2. Mean Global Annual Runoff Distribution for the period 1986–1995 per 1° latitudinal band as simulated by LPX and as represented by the ISLSCP II composite dataset. Freshwater extractions for 1995 are based on Oki et al. (2001).

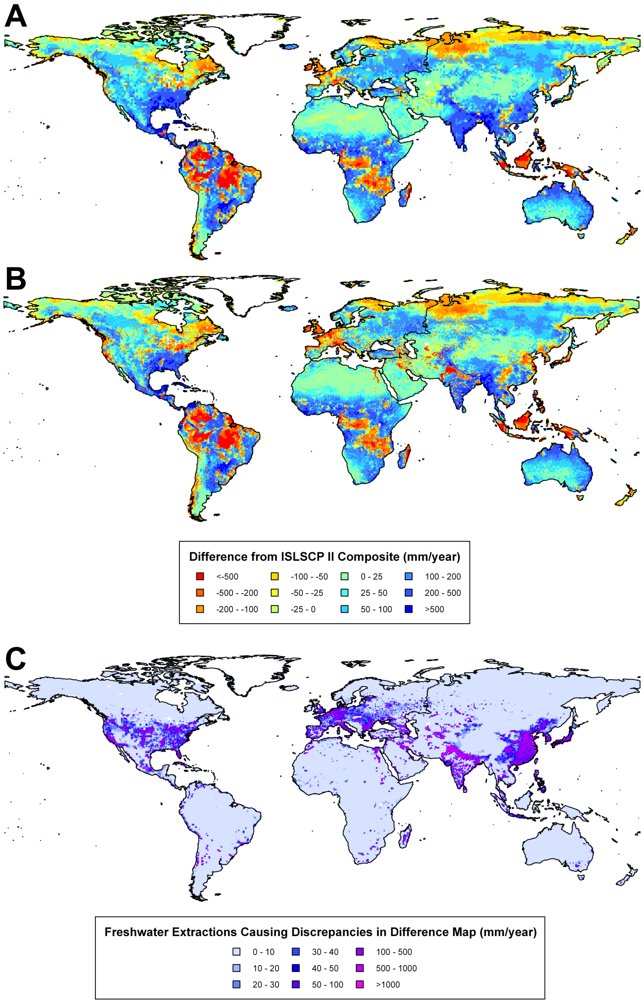
A
B
Difference from ISLSCP II Composite (mm/year)
<-500
-500 - -200
-200 - -100
-100 - -50
-50 - -25
-25 - 0
0 - 25
25 - 50
50 - 100
100 - 200
200 - 500
>500
C
Freshwater Extractions Causing Discrepancies in Difference Map (mm/year)
0 - 10
10 - 20
20 - 30
30 - 40
40 - 50
50 - 100
100 - 500
500 - 1000
>1000

Fig. 3.

Fig. 3. (A) Difference in LPX mean annual runoff (mm/year) from the ISLSCP II composite dataset for the period 1986–1995 **(B)** Difference in mean annual runoff for LPX and ISLSCP II (1986–1995) with 1995 annual freshwater extractions totals incorporated (mm/year; based on Oki et al. 2001) **(C)** Difference between former two figures to highlight regions where freshwater extractions (mm/year) are important in influencing the discrepancies between LPX and ISLSCP II runoff estimates.

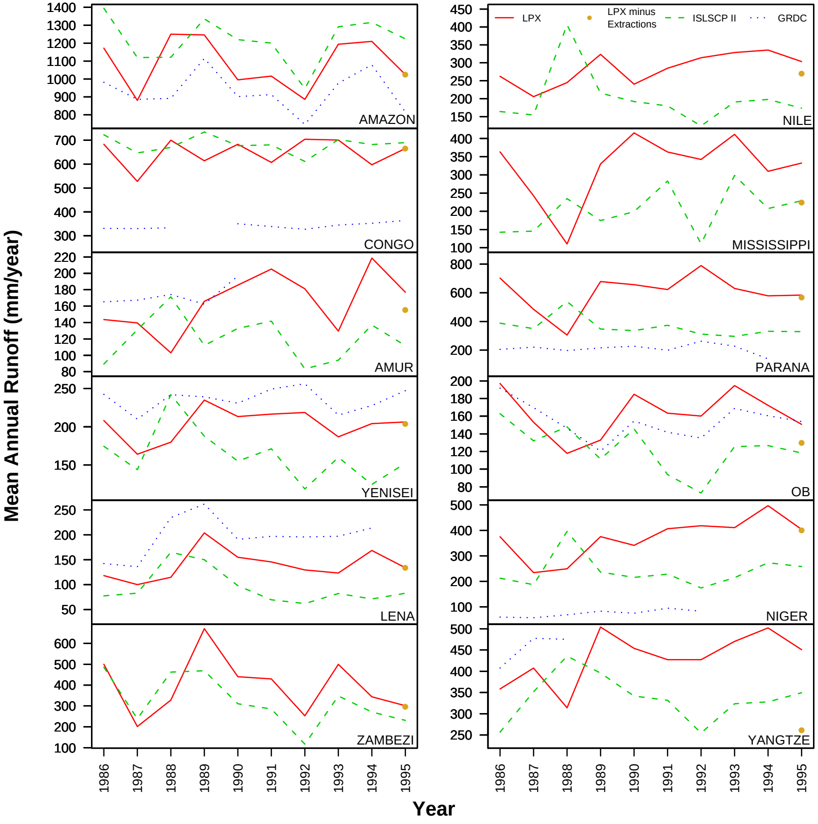

Fig. 4. Interannual variability in mean annual runoff for twelve selected catchments as represented by LPX, the ISLSCP II composite data and, where available, GRDC disaggregated river discharge observations. LPX simulated runoff with freshwater extractions for 1995 are also shown.

Title Page
Abstract
Introduction
Conclusions
References
Tables
Figures
◀◀
▶▶
◀
▶
Back
Close
Full Screen / Esc
Printer-friendly Version
Interactive Discussion

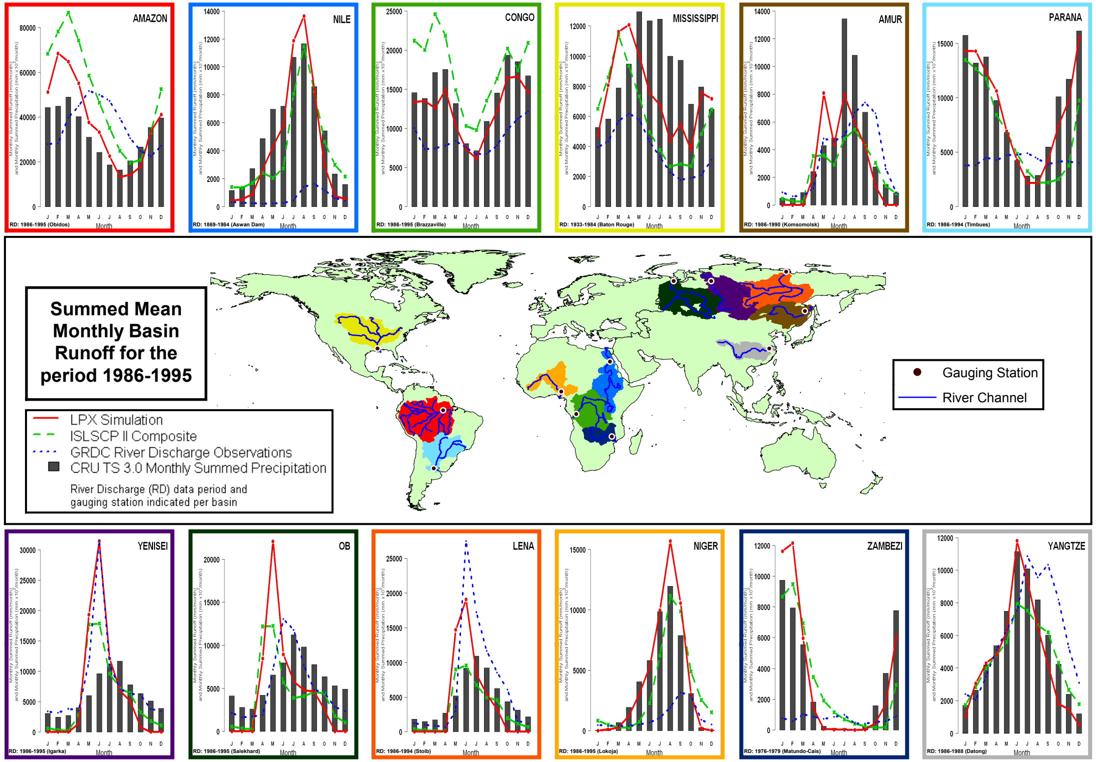

Fig. 5. Summed monthly catchment runoff averaged for 1986–1995 as represented by LPX, the ISLSCP II composite data and GRDC disaggregated mean monthly river discharge observations converted to runoff equivalent. Also shown are CRU TS 3.0 monthly summed precipitation observations.

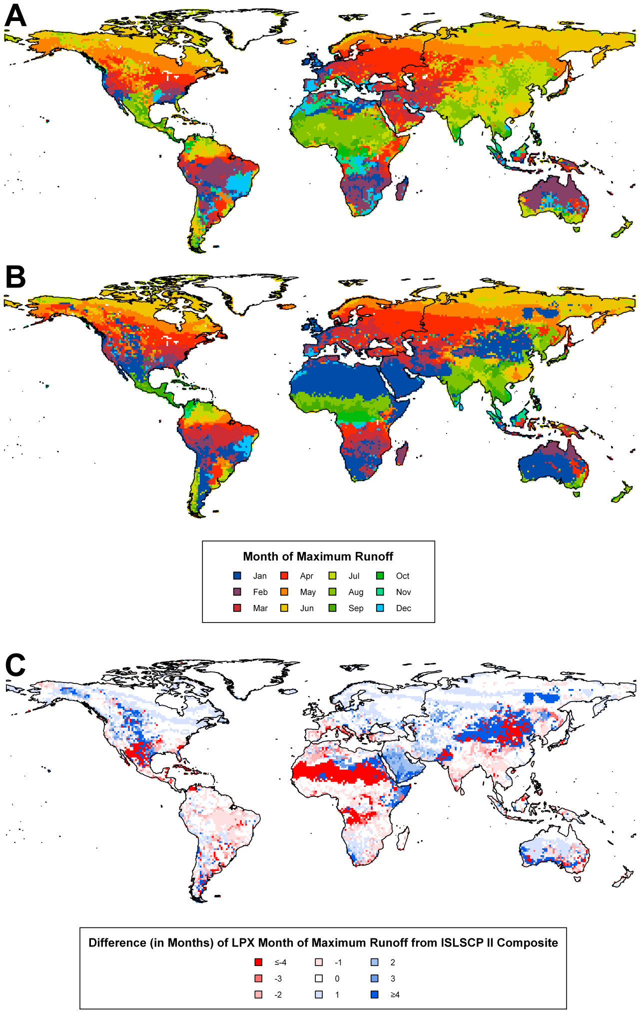
A
B
Month of Maximum Runoff
Jan
Feb
Mar
Apr
May
Jun
Jul
Aug
Sep
Oct
Nov
Dec
C
Difference (in Months) of LPX Month of Maximum Runoff from ISLSCP II Composite
≤-4
-3
-2
-1
0
1
2
3
≥4

Fig. 6.

Fig. 6. **(A)** Month of maximum runoff as simulated by the LPX-DGVM. **(B)** Month of maximum runoff for as represented by the ISLSCP II composite dataset. **(C)** Difference in months between month of maximum runoff of LPX from the ISLSCP II composite dataset.

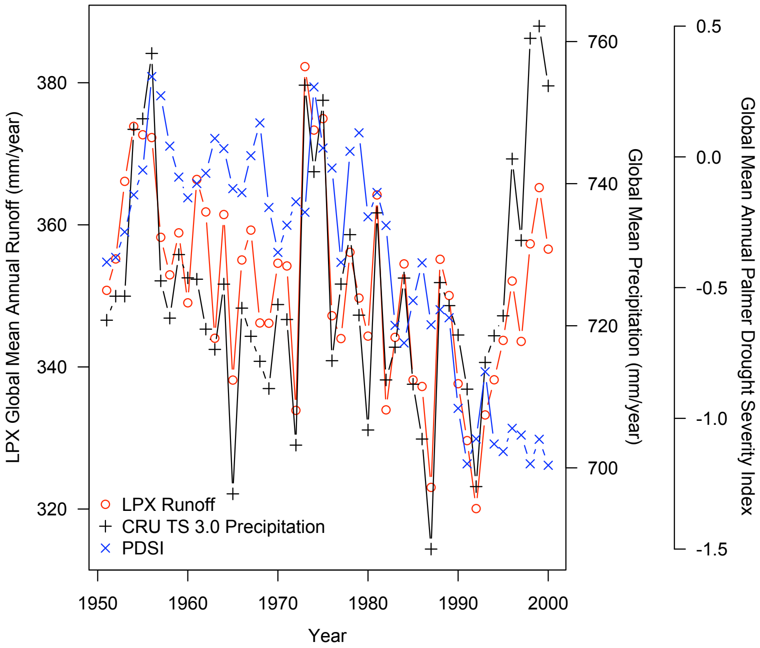

Fig. 7. Global Mean Annual Runoff as simulated by LPX versus Global Mean Annual Palmer Drought Severity Index (PDSI) and Global Mean Precipitation.

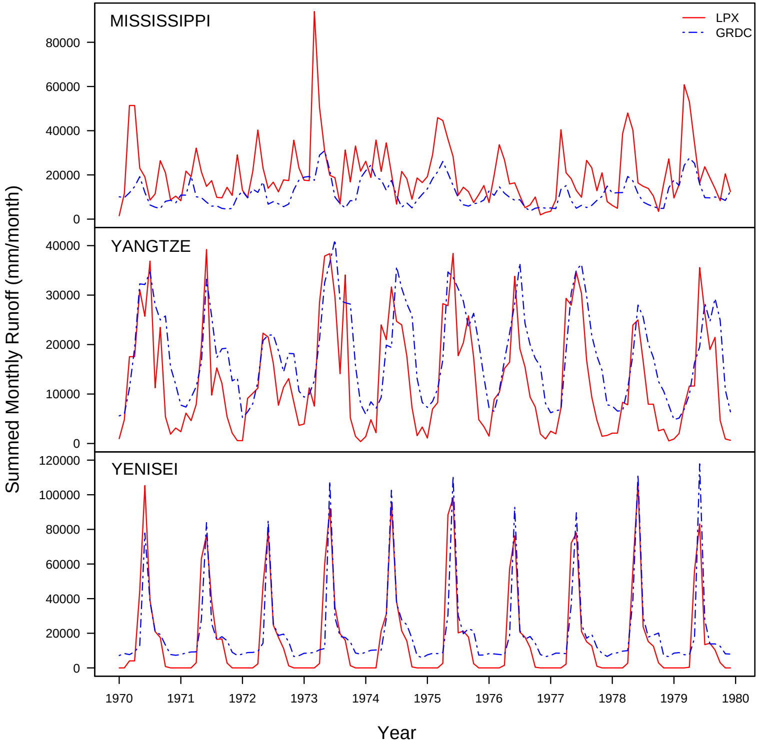

Fig. 8. Total summed monthly catchment LPX runoff versus GRDC runoff equivalent river discharge for the Mississippi, Yangtze and Yenisei catchments (1970–1979).

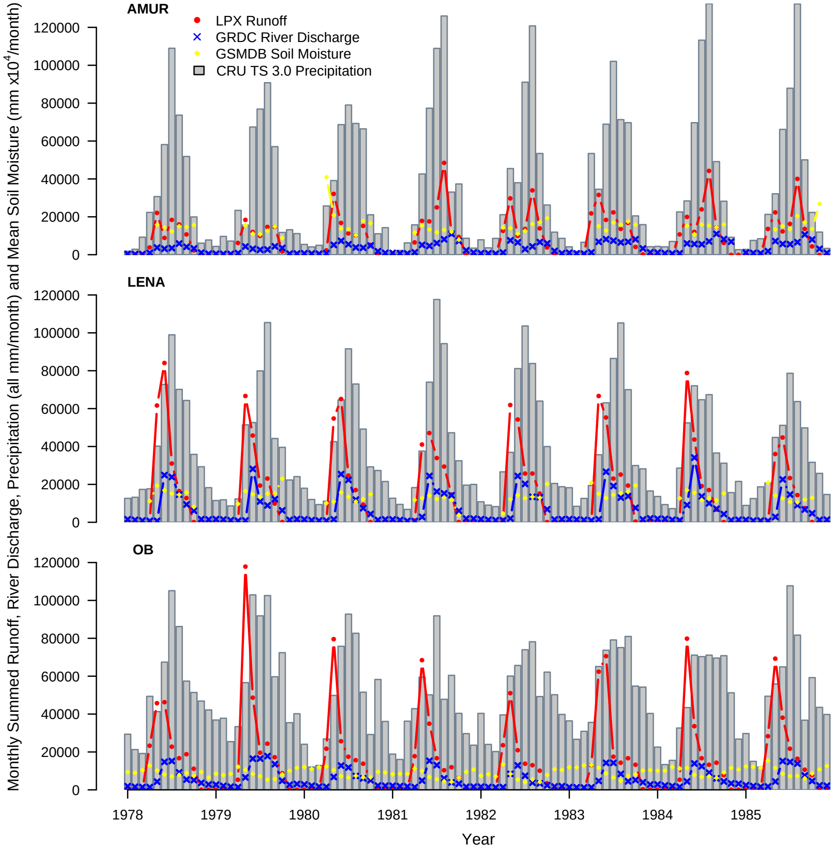

Fig. 9. Monthly summed catchment LPX runoff, CRU TS 3.0 precipitation, GRDC river discharge (all mm/month) and Global Soil Moisture Data Bank soil moisture (mm × 10^4/month) for the Amur, Lena and Ob catchments.